Temperature-dependent photoluminescence of organic semiconductors with varying backbone conformation

S. Guha,[1,*] J. D. Rice,[1] Y. T. Yau,[1] C. M. Martin,[2] M. Chandrasekhar,[2] H. R. Chandrasekhar,[2] R. Guentner,[3] P. Scanduicci de Freitas,[3] and U. Scherf[3]

[1]*Department of Physics, Astronomy and Materials Science, Southwest Missouri State University, Springfield, Missouri 65804*

[2]*Department of Physics, University of Missouri, Columbia, Missouri 65211*

[3]*Institut für Chemie and Polymerchemie, Universität Potsdam, Germany*

(Received 18 June 2002; revised manuscript received 5 August 2002; published 17 March 2003)

We present photoluminescence studies as a function of temperature from a series of conjugated polymers and a conjugated molecule all with distinctly different backbone conformations. The organic materials investigated here are planar methylated ladder-type poly *para*-phenylene, semi-planar polyfluorene, and nonplanar *para*-hexaphenyl. In the long-chain-polymers the photoluminescence transition energies blueshift with increasing temperatures. In contrast, in the conjugated molecules transition energies redshift with increasing temperatures. Empirical models that explain the temperature dependence of the band gap energies in inorganic semiconductors are extended to explain the temperature dependence of the transition energies in conjugated molecules.

DOI: 10.1103/PhysRevB.67.125204 PACS number(s): 78.55.Kz, 68.60.Dv, 42.70.Jk

I. INTRODUCTION

Conjugated organic semiconductors such as short-chain oligomers and long-chain polymers are very promising active materials for low-cost, large-area optoelectronic and photonic devices.[1] Semiconducting properties are defined by the ability of these materials to efficiently transport charge (holes or electrons) along the chain due to their π-conjugation or between adjacent chains due to the π-orbital overlap of neighboring molecules. Commercial availability of organic light-emitting diodes (OLED) has attracted growing attention to π-conjugated molecules such as oligothiophene, oligomers of poly *para*-phenylene (PPP), and polymers[2,3] such as poly *para*-phenylene vinylene (PPV), polythiophene, PPP, and polyfluorene (PF).[4]

In recent years PFs have emerged as attractive alternatives, showing the highest photoluminescence quantum efficiency (55%) compared to other conjugated polymers/molecules in solid state[5] and also maintain a high hole mobility at room temperature.[6] Since high photoluminescence quantum yield (PLQY) is the primary consideration in devices such as OLED, mechanisms that change the PLQY are crucial to the understanding and design of these devices. Temperature-dependent photoluminescence (PL) studies[7–11] help determine the stability of conjugated polymers and molecules in devices, and to understand how the optical processes change.

In this work we compare the steady-state temperature-dependent PL from three families of organic semiconductors that show a strong blue luminescence. Blue electroluminescent materials are of particular interest for organic displays since blue light can easily be converted into red and green by color-changing media (fluorescent dyes). To probe the origin of the changes in the PL energies with temperature, we investigate three families of materials that include two long-chain polymers, methylated ladder-type PPP and polyfluorene, and one short-chain polycrystalline oligomer. The ladder-type polymer has a very rigid backbone conformation with almost no torsional degree of freedom, the oligomer has a very high torsional degree of freedom, and PF has a backbone conformation intermediate to the ladder-type polymer and the oligomer. The structural differences in these materials allow us to probe the following two questions regarding the temperature dependence of their electronic states: whether there is any difference between the long-chain and the short-chain conjugated molecules and if the torsions (owing to the different backbone conformations) play a role in this process.

The temperature dependence of electronic states in *inorganic* semiconductors and heterostructures has been studied extensively in the last few decades. In these systems the band gaps exhibit large shifts and changes in their lifetime induced broadenings as a function of temperature.[12] One of the first empirical models to explain the temperature dependence of the band gap energy in bulk semiconductors was put forward by Varshni.[13] Subsequently, there have been other empirical models that apply an average Bose-Einstein statistical factor for phonons to explain the temperature dependence of the electronic states.[14,15] The latter approach is more suitable for the temperature dependence of the transition energies in narrow-well inorganic semiconductor heterostructures and superlattices.[16]

In inorganic semiconductors the two mechanisms that are responsible for the temperature dependence of energy bands at constant pressure are thermal expansion and renormalization of band energies by electron-phonon interactions. Typically the former mechanism has a negligible effect so that the changes in the band gap energies arise primarily from electron-phonon interactions. Theoretical calculations of the temperature dependence of band energies in Si and Ge that take into account such electron-phonon interactions agree very well with the experimental results.[17] In this work we test the extension of existing models for inorganic semiconductors to organic materials and find a good agreement of the model to the short-chain oligomers.

This paper is organized as follows: Sec. II describes the structural properties of the organic semiconductors and the experimental setup. In Sec. III, we present the PL results

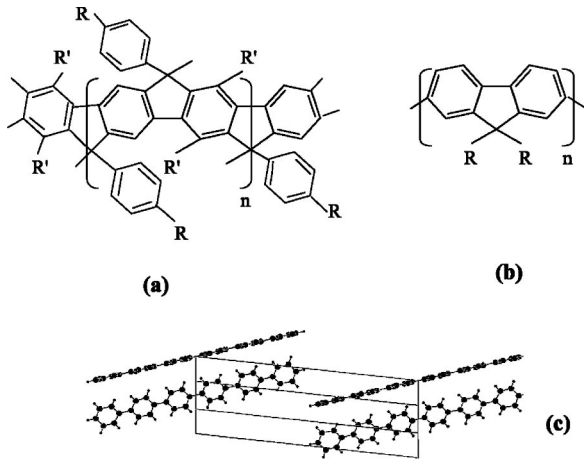

FIG. 1. Chemical structure of (a) MeLPPP, (b) PF2/6, and (c) PHP. In (a) R and R' refer to $C_{10}H_{21}$ and C_6H_{13}, respectively, and in (b) R refers to the ethyl hexyl side chain.

from methyl substituted ladder type poly *para*-phenylene (MeLPPP), PF, and *para* hexaphenyl (PHP) as a function of temperature. Section IV is a discussion of our results, followed by our conclusions in Sec. V.

II. EXPERIMENTAL DETAILS

A. Structural properties

The three families of conjugated materials that we compare in this work include non-planar PHP, planar MeLPPP, and semiplanar poly(2,7-[9,9′-bis(2-ethylhexyl)]) fluorene (PF2/6). All three materials are of technological importance due to their strong blue luminescence and high chemical purity, and have been used as active materials in OLED.[5,18,19] Both MeLPPP and PF2/6 are long-chain processable conjugated polymers,[20] whereas PHP is a short-chain oligophenyl that forms monoclinic crystallites of space group $P2_1/a$.[21]

PHP is characterized by a torsional degree of freedom between neighboring phenyl rings. In the crystalline state the molecules are arranged in layers, with a herringbone type arrangement found in each layer as shown in Fig. 1(c). PHP can be planarized by the application of hydrostatic pressure.[22] On the average, at room temperature it is more planar than at lower temperatures.[21]

MeLPPP is amorphous due to the bulky side groups. Neighboring phenyl rings are planar due to the methyl bridges and show no torsional degree of freedom [see Fig. 1(a)]. The planarity between phenyl rings results in a high intrachain order and a low defect concentration. This is attributed to the synthesis method, which is highly selective in forming only certain bonds, and hence reduces the number of defects.[23]

PF2/6, on the other hand, can be viewed as a semiplanar polymer, with a backbone conformation somewhere in between that of MeLPPP and PHP. It forms planar monomer units but has a torsional degree of freedom between adjacent monomer units, as shown in Fig. 1(b). The alkyl side chains of the fluorene moieties have been shown to strongly influence the solid-state packing of the molecule.[24]

We also compare the spectra of two other derivatives of polyfluorene: a dialkylated copolymer, poly[9,9-bis(3,7,11-trimethyldodecyl)fluorene-2,7-diyl] (PF1112), and poly (9,9-bis[4-(2-ethylhexoxy)phenyl] fluorene) (PF-P). The copolymer has longer alkyl side chains compared to PF2/6 with 2% of 2,7-fluorenone units incorporated in the backbone as a model for a photodegeneration-induced defect-rich polyfluorene. PF-P is a diphenyl-substituted PF exhibiting an extraordinarily small defect concentration.

Upon further processing some polyfluorene films display a β phase, which has a more extended intrachain π-conjugation, in addition to the regular glassy α phase. The β phase has been detected in 9,9-di-*n*-octyl-PF (PF8 or PFO) upon thermal cycling from 80 to 300 K (Ref. 25) and slowly reheating it to room temperature or exposing a film to the vapor of a solvent.[26] The β phase shows a distinct redshift of absorption and emission peaks with a well-resolved vibronic progression both in absorption and emission. In contrast, the α phase shows a well-resolved vibronic progression only in the emission spectrum. Using x-ray and electron diffraction measurements, Lieser *et al.* have shown that the β phase is completely absent in PF with branched side groups like PF2/6.[27]

B. Methodology

PL spectra were measured from films of MeLPPP, PF, and PHP. The MeLPPP and PF2/6 films were prepared by spin coating on a glass slide from a toluene solution, and their thickness was 0.1 μm. We also prepared a thicker film ($\sim$3 μm) by dropcasting PF2/6. In this paper PF(A) and PF(B) refer to the thick and thin PF2/6 films, respectively. The films were dried at room temperature. Highly purified PHP was obtained from Tokyo Chemical Industries, Ltd. The PHP film was prepared by vacuum evaporation (10^{-6} mbar) on regular glass substrates. The thickness of the sample was $\sim$0.1 μm. The PL spectra were excited using the 363.8 nm line of an Ar^+ laser. The luminescence excitation was analyzed with a SPEX 0.85 m double monochromator equipped with a cooled GaAs photomultiplier tube and standard photon counting electronics. The samples were loaded in a cryostat and evacuated to below 100 mTorr to prevent photo-oxidative damage. For low temperature measurements a closed cycle refrigerator was employed.

III. PL RESULTS

A vibronic progression is seen in the PL emission for all the materials under consideration, indicating a coupling of the backbone carbon-carbon stretch vibration to electronic transitions. The vibronic spacing in all the samples lies between 1300 and 1400 cm^{-1}. The vibronic peaks result from a nonzero overlap of different vibronic wave functions of the electronic ground and excited states. The emissive transition highest in energy is called the 0-0 transition, which takes place between the zeroth vibronic level in the excited state and the zeroth vibronic level in the ground state. The 0-1 transition involves the creation of one phonon. In the adiabatic picture, vibronic progression in the electronic spectra

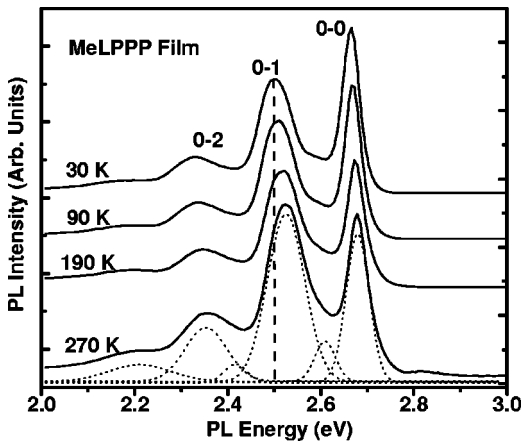

FIG. 2. PL spectra of a MeLPPP film at a few values of temperature. The dotted line under the 270 K data shows the actual fit to the data. The vertical dashed line indicates a blueshift of the 0-0 vibronic peak with increasing temperature.

implies that the ground and excited state equilibrium structures are displaced relative to one another in configuration space. Additional vibronic replicas are also observed in between the main vibronic peaks, representing some of the weaker phonon modes coupling to the electronic transitions.

A. MeLPPP film

Figure 2 shows the PL spectra of an MeLPPP film at a few selected values of temperature. The PL spectrum was fitted with Gaussians in order to obtain the individual peak positions, amplitudes, and broadening [full width at half maximum (FWHM)] parameters. The three main vibronic peaks observed are labeled as the 0-0, 0-1, and the 0-2. There are additional vibronic peaks observed between the main vibronic peaks that are also seen in other works.[28] The dotted line under the 270 K spectrum is a representative of our fits. At 30 K the main vibronic peaks that are observed are the 0-0 peak at 2.67 eV, the 0-1 at 2.5 eV, 0-2 vibronic peak at 2.33 eV, and the 0-3 peak at 2.19 eV. In addition, vibronic replicas are observed at 2.61 eV and 2.4 eV. The energy difference between the main successive vibronic peaks is 0.17 eV, indicative of the coupling of carbon-carbon stretch vibration to the conjugated backbone. At all temperatures the PL spectra were fitted with the same number of Gaussian peaks for consistency. The overall spectrum not only blueshifts with increasing temperatures but the relative intensities of the individual vibronic peaks change as well.

Figure 3(a) shows the energy position of the 0-0 and the 0-1 vibronics as a function of temperature. The 0-2 peak in MeLPPP shows a similar behavior. The average value of the rate of shift is $7.5\times10^{-5}\pm0.1$ eV/K. Figure 3 (b) shows the FWHM (eV) for the 0-0 and the 0-1 vibronic peaks as a function of temperature. The linewidths decrease between 300 K and 100 K and then increase below 100 K. This cannot be attributed to any fitting artifact: at all temperatures the PL spectrum is fitted with same number of individual vibronic peaks (shown in the 30 K data of Fig. 2) which are

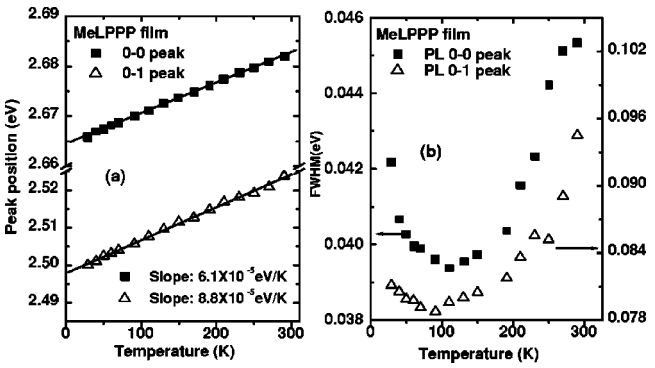

FIG. 3. (a) The peak position of the 0-0 and the 0-1 PL transitions as a function of temperature in MeLPPP (b) FWHM of the 0-0 and the 0-1 peak as a function of temperature in MeLPPP.

allowed to vary in position, amplitude, and width till the best fit is obtained. Moreover, both the 0-0 and the 0-1 vibronic peaks show the same trend.

B. PF film

Figure 4 shows the PL spectra from two PF2/6 films (with different thickness) for a few selected values of temperature. The relative intensity of the 0-0 peak to the 0-1 peak in PF(A) (thick film), is lower compared to PF(B) (thin film) indicating a higher self-absorption in PF(A). At 24 K the main vibronic peaks that are observed are the 0-0 peak at 2.93 eV, the 0-1 at 2.77 eV, and the 0-2 transition at 2.59 eV in PF(B). An additional vibronic replica is observed at 2.86 eV between the 0-1 and 0-2 peaks. The PL transition energies show a blueshift with increasing temperature, similar to the MeLPPP sample. The peak positions and the FWHM of the 0-0 and the 0-1 PL vibronics are shown in Fig. 5. The sublinear behavior of the 0-0 peak position in PF(B) with increasing temperature may be related to self-absorption effects.

The PL spectra of PF(A) show a slightly different behavior, as seen in Fig. 4(a). The 0-0 peak redshifts whereas the

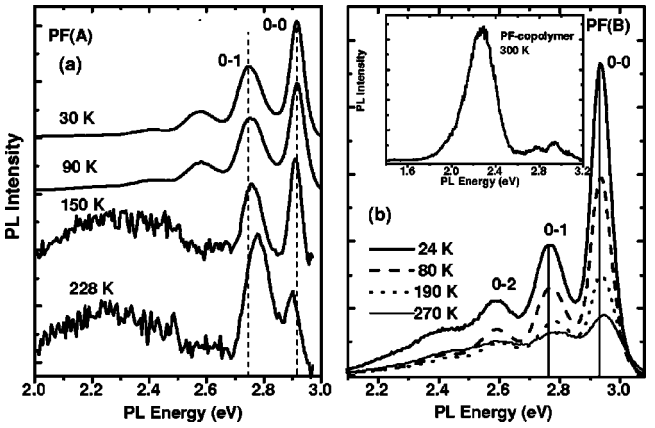

FIG. 4. PL spectrum of PF2/6 at selected values of temperature for a (a) thicker and (b) thinner film. The vertical lines show the shift in the transition energies with temperature. The inset in (b) is the PL spectrum of PF copolymer at 300 K. The strong 2.3 eV peak is related to the emission from the keto defects.

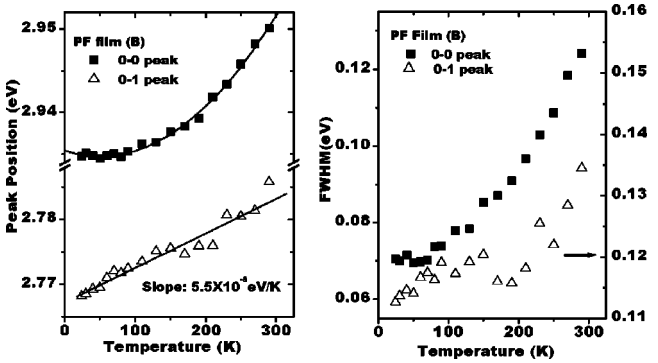

FIG. 5. (a) Peak position of the 0-0 and the 0-1 peak in PF(B) as a function of temperature. (b) FWHM of the 0-0 and the 0-1 peak in PF(B) as a function of temperature.

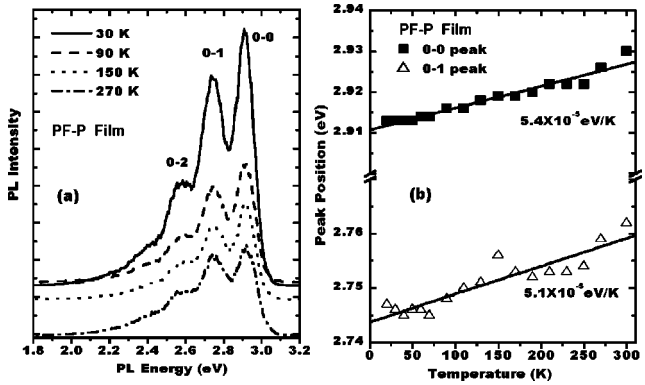

FIG. 6. (a) PL spectra of PF-P at a few values of temperature. (b) The 0-0 and the 0-1 peak position as a function of temperature in PF-P.

0-1 peak blueshifts with increasing temperatures. The redshift of the 0-0 peak in this sample is most probably an artifact due to self-absorption effects. With increasing temperature a broad peak at 2.3 eV emerges at around 150 K, shown in Fig. 4(a). Recent work suggests that this peak is related to the emission from keto defects sites (9-fluorenone sites).[24,29] These defect sites act as guest emitters that can efficiently trap singlet excitons created on the conjugated polyfluorene backbone by a dipole-dipole induced Förster-type energy transfer.[30] The keto defect sites can be accidentally incorporated into the π-conjugated PF backbone due to the presence of nonalkylated or monosubstituted fluorene sites during synthesis or as a result of a photo-oxidative degradation process. In order to reduce photodegradation due to the exciting UV, the samples were kept in vacuum during our PL measurements. The concentration of these defect sites is quite low in the PF2/6 sample since the 2.3 eV emission is absent in the thinner PF(B) film. Also, it is a thermally activated process; in PF(A) the defect related emission is only observed for temperatures above 150 K. The inset of Fig. 4(b) shows the PL spectrum from PF1112, the copolymer with 2% incorporated fluorenone sites. The strong 2.3 eV emission is from the keto defects which overwhelms the emission from the PF backbone.

In contrast, the diphenyl-substituted PF (PF-P) is expected to have almost no keto defects due to a different synthesis of the corresponding monomer blocks that prevents non- or monosubstituted fluorene sites. We compare the temperature dependent PL from a drop-casted film of PF-P to the PF2/6 sample of film thickness comparable to the sample PF(A). Figure 6(a) shows the PL spectra from PF-P for selected values of temperature. Clearly the 2.3 eV emission is not observed at higher temperatures unlike in PF(A), indicating that the sample is almost free of keto defect sites. Figure 6(b) shows the peak position of the 0-0 and the 0-1 vibronics as a function of temperature. The average value for the rate of shift of the PL vibronics is $5.2\times10^{-5}\pm0.3$ eV/K.

C. PHP

The PL measurements from PHP were measured both from the powder and from a thin evaporated film. Figure 7 shows the PL spectra both from the powder and film for selected temperatures. The 0-0 transition is not observed in the powder due to self-absorption. The film also shows a certain amount of self-absorption since the relative intensity of the 0-0 peak is smaller compared to the 0-1 or the 0-2 transition peak. At 30 K the main vibronic peaks that are observed are the 0-0 peak at 3.12 eV, the 0-1 at 2.95 eV, and the 0-2 vibronic peak at 2.78 eV. Additional vibronic peaks are observed at 3.07 eV and 2.86 eV. The individual vibronics redshift with increasing temperatures both in the film and powder. A redshift of the PL spectrum with increasing temperatures in PHP has been observed before, but a detailed analysis was not carried out.[22,31] The PHP film was more prone to local heating effects during the PL measurement; we therefore restrict our analysis of the PL energy shifts to the PHP powder. Figures 8(a) and 8(b) show the individual positions of the 0-1 and the 0-2 peaks, respectively, from the PHP powder. The bold line is a fit to an empirical model, discussed in detail in Sec. IV.

IV. DISCUSSION

Conjugated polymers can be viewed as an inhomogeneous collection of varying-length chain segments. Time- and frequency-resolved optical studies show that after a photon excites a chain segment with energy above the threshold, the exciton that is created executes a random walk through

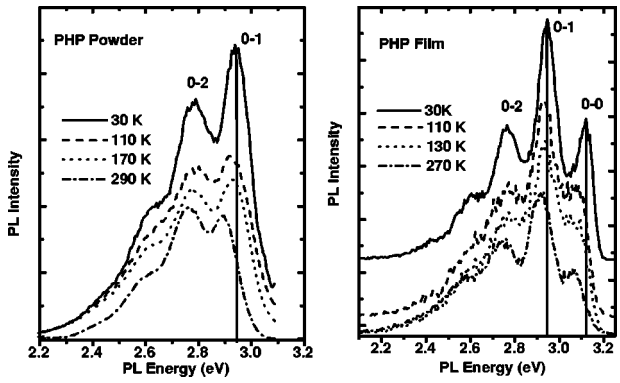

FIG. 7. PL spectra at four selected values of temperature for (a) PHP powder and (b) a thin evaporated PHP film.

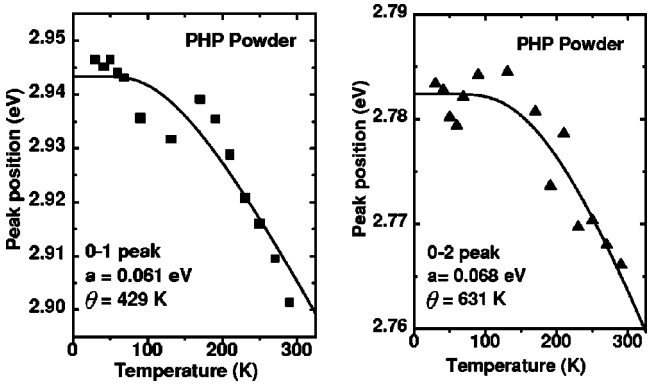

FIG. 8. Peak position of the (a) 0-1 and the (b) 0-2 PL transition energies from PHP powder as a function of temperature. The bold line is a fit to Eq. (3).

the density of states via Förster energy transfer,[30] until it becomes trapped on a low-energy site, from where emission occurs. These sites presumably have a higher conjugation length.[7,32]

The temperature dependence of the PL energies is different for long-chain conjugated polymers compared to the shorter chain oligomers; conjugated polymers show a blueshift of PL energies with increasing temperatures, whereas conjugated molecules like PHP show a redshift with increasing temperature. We point out that although the two types of polymers have different backbone conformation (MeLPPP is planar, PF2/6 is semiplanar), both show the same trend as a function of temperature. A similar blueshift in PL energies with increasing temperature has been observed in other conjugated polymers such as PPV[7–9] and MEH-PPV,[10,11] and has typically been attributed to lattice fluctuations.

A. Huang-Rhys factor

The spectral intensity is approximated by the superposition of transitions between the vibrational frequencies of the ground and the excited electronic states. In the emission process the probability of the 0th vibronic excited state to the nth vibronic ground state is given by

$$I_{0\to n}=\frac{e^{-S}S^{n}}{n!}, \tag{1}$$

where $S=M\omega/2\hbar\Delta^{2}$ is the Huang-Rhys factor.[33] Here ω is the vibrational frequency, M is the reduced mass of the harmonic oscillator that couples to the electronic transition, and Δ is the displacement of the potential curve between the ground and excited electronic states. The Huang-Rhys factor therefore corresponds to the average number of phonons that are involved when the excited molecule relaxes from its ground state configuration to the new equilibrium configuration in the excited state (after the absorption of a photon) and $S\hbar\omega$ is the relaxation energy. If we assume that ω is the same for ground and excited states and that the potentials are perfectly parabolic, S can be determined from the fractional intensity of the vibronic peaks:

$$S=(I_{0\to1}+2I_{0\to2}+3I_{0\to3})/I_{\text{total}}. \tag{2}$$

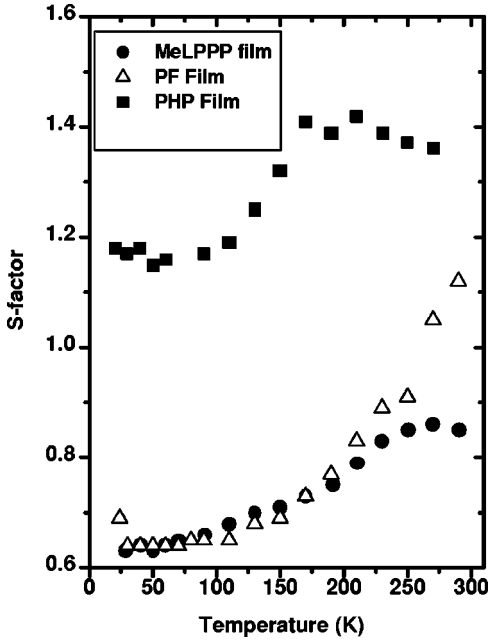

FIG. 9. Huang-Rhys factor versus temperature for MeLPPP, PF2/6, and PHP films. S was calculated using Eq. (2).

$I_{0\to1}$, $I_{0\to2}$, and $I_{0\to3}$ refer to the intensity of the emission from the zeroth vibrational level excited state to the first, second, and third vibrational level of the ground state, respectively. I_{total} is the total intensity of the individual vibronics. Here we assume that the transition matrix elements are the same for all vibronics and neglect all vibronics above 0-3.

The relative strengths of the vibronic transitions also change along with shifts in energy with temperature. The Huang-Rhys factor decreases both for the polymers and PHP with decreasing temperature, as shown in Fig. 9. The S factor was calculated using Eq. (2). Smaller molecules exhibit a larger S factor due to their large normal coordinate displacements (for a detailed explanation see Hagler *et al.*[10]). It is therefore not surprising that PHP has a higher S factor compared to the polymers. From Fig. 9 it is seen that PHP shows a saturation effect at higher temperatures. This may be related to the fact that since the electronic transition energies redshift with increasing temperatures, there may be a higher overlap of the 0-0 peak with absorption resulting in a further decrease in the intensity of the 0-0 peak in addition to the effect of temperature.

A decrease in S with decreasing temperature has been observed in other works and is interpreted as an effect arising from increased conjugation due to exciton delocalization.[7] This picture by itself cannot explain the temperature dependence of the PL from both the conjugated polymers and the shorter molecules, since PHP clearly shows a redshift of transition energies with increasing temperatures. We also observe the PL emission from quaterphenyl powder, which is a short-chain oligomer to redshift with increasing temperatures. Therefore we must really look at these systems separately: the conjugated polymers that have a distribution of chain lengths and the shorter molecules that have more or less the same chain length distribution. Lattice fluctuations

change as a function of temperature for all three materials as indicated by the change in the *S* factor but they do not address the issue of the difference in the shifts of the PL for the oligomers versus the polymers.

B. Redshift versus blueshift

The electronic energies in bulk inorganic semiconductors display temperature dependence mainly due to renormalization of band energies by electron-phonon interactions. The temperature dependence of the interband transitions is mainly due to the interactions of the exciton with relevant acoustical and optical phonons. It can be described with an expression in which the energy thresholds decrease proportional to the Bose-Einstein statistical factors for phonon emission plus absorption[14]

$$E_g(T) = E(0) - \frac{2a}{[\exp(\Theta/T) - 1]}, \tag{3}$$

where $E(0)$ is the band gap energy at 0 K, and a is the strength of the exciton-phonon interaction. This includes contribution both from the acoustical and optical phonons. Θ is the average phonon temperature. By fitting the 0-1 and the 0-2 PL vibronics of PHP with Eq. (3) (see Fig. 8), we obtain an average $a = 0.065 \pm 0.01$ eV and an average $\Theta = 530 \pm 150$ K. These values are comparable to other inorganic semiconductors, for example in bulk GaAs, $a = 0.057$ eV, and $\Theta = 240$ K. A higher value of Θ implies a smaller contribution from the acoustic phonons, and should also result in a stronger exciton-phonon interaction. It is not surprising that PHP has a higher value of Θ compared to that of GaAs since the optical phonons due to the carbon-carbon stretch modes have much higher energies compared to the optical phonons in GaAs. The PL linewidth of the individual vibronics in PHP show a scatter with increasing temperature and on the average remains a constant.

Although the polymers, MeLPPP, PF2/6, and PF-P, all show a blueshift of their PL energies with increasing temperatures, they shift at slightly different rates. The PL vibronics in MeLPPP shift at the rate of $7 \times 10^{-5} \pm 0.1$ eV/K [Fig. 3(a)]. The PL energies in PF2/6 and PF-P shift at similar rates of $5 \times 10^{-5} \pm 0.4$ eV/K [Figs. 5(a) and 6(b)]. The slightly different rates in MeLPPP and PF-type polymers may have to do with the differences in their conjugation length, especially since their molecular weights are not that different. PF2/6 and PF-P show a broadening of the PL linewidths with increasing temperatures. Beyond 100 K, MeLPPP shows a broadening of the PL linewidths, as seen in Fig. 3(b). The line narrowing of the 0-0 and the 0-1 peak at 100 K in MeLPPP is not completely understood.

A blueshift of the PL energies with increasing temperature from the two families of the conjugated polymers with planar backbone confirmation (MeLPPP) and semiplanar backbone confirmation (PF2/6 and PF-P) confirms the Bässler-Schweitzer[33] argument that the process should not really depend upon the torsional fluctuations. Otherwise, MeLPPP, which has a planar backbone conformation, should show a different behavior. The shifts in the PL energies reflect more on the temperature dependence of the relaxation process. A plausible explanation is that upon increasing the temperature, the excitons that are created on the polymer backbone do not easily migrate to the low energy segments; they remain localized on the shorter-chain segments that have higher energies. This is in agreement with the time-resolved PL measurements of PPV at 20 K and 300 K by Lim *et al.*[7] The spectral shift to lower energies at 300 K is 50% smaller compared to the 20 K measurement. This suggests that at higher temperatures there are fewer stationary, low energy trap sites, and the exciton remains more localized on a smaller segment.

In PHP the main contribution to the temperature dependence of electronic energy arises from the exciton-phonon interaction term, similar to that in inorganic semiconductors. A possible scenario is that in the long-chain polymers both renormalization of band energies due to electron-phonon interaction as well as prevention of energy migration to lower energy sites play a role, and the latter appears to be dominant.

We mention that in inorganic semiconductors such as GaN quantum dots (QD's),[34] where there is a distribution of the dot size, the PL energies blueshift with increasing temperature, similar to the conjugated polymers. Increasing temperatures result in a preferential loss of carriers from larger QD's (which have lower energies), resulting in a net blueshift of the transition energy due to the emission from the smaller dots. This is in contrast to bulk GaN,[35] where the band energies redshift with increasing temperatures.

V. CONCLUSION

We have presented systematic temperature-dependent steady-state PL studies from a series of conjugated polymers and a molecule with variations in their backbone conformations. The conjugated polymers show a blueshift of their PL transition energies with increasing temperature, independent of their actual backbone conformation. MeLPPP, which is planar, and PF, which has a semiplanar backbone confirmation, show a similar trend in their PL energies as a function of temperature. The shifts in the electronic energies reflect on the temperature dependence of the actual relaxation process whereby the exciton remains more localized on smaller chain segments on increasing the temperature.

The shorter conjugated molecule, PHP, which has a similar distribution of chain lengths, shows the opposite trend: a redshift of the transition energies with increasing temperature, indicating a renormalization of band energies due to electron-phonon interaction. This behavior is similar to that observed in bulk inorganic semiconductors and can be described by an empirical model that takes into account the Bose-Einstein statistical factors for phonon emission and absorption.

ACKNOWLEDGMENTS

The work at SMSU was partly funded by the Research Corporation Grant No. CC5332 and the Petroleum Research Fund Grant No. 35735-GB5. S.G. would also like to acknowledge the SMSU summer faculty support and the Faculty Research Grant. U.S. thanks SONY International Europe, Stuttgart, and the Deutsche Forschungsgemeinschaft (DFG) for financial support.

*Author to whom correspondence should be addressed. Electronic address: sug100f@smsu.edu

[1] For a review see J.M. Shaw and P.F. Seidler, IBM J. Res. Dev. **45**, 3 (2001); *Handbook of Conducting Polymers*, edited by T.A. Skotheim, R.L. Elsenbaumer, and J.R. Reynolds (Marcel Dekker, New York, 1998).

[2] J.H. Burroughes, D.D.C. Bradley, A.R. Brown, R.N. Marks, K. Mackay, R.H. Friend, P.L. Burns, and A.B. Holmes, Nature (London) **347**, 539 (1990).

[3] Y. Ohmori, M. Uchida, K. Muro, and K. Yoshini, Jpn. J. Appl. Phys., Part 2 **30**, L1938 (1989).

[4] M.T. Bernius, M. Inbasekaran, J. O'Brien, and W. Wu, Adv. Mater. **12**, 1737 (2000).

[5] A.W. Grice, D.D.C. Bradley, M.T. Bernius, M. Inbasekaran, W.W. Wu, and E.P. Woo, Appl. Phys. Lett. **73**, 629 (1998).

[6] M. Redecker, D.D.C. Bradley, M. Inbasekaran, and E.P. Woo, Appl. Phys. Lett. **73**, 1565 (1998).

[7] S-H. Lim, T.G. Bjorklund, and C.J. Bardeen, Chem. Phys. Lett. **342**, 555 (2001).

[8] N.T. Harrison, D.R. Baigent, I.D.W. Samuel, R.H. Friend, A.C. Grimsdale, S.C. Moratti, and A.B. Holmes, Phys. Rev. B **53**, 15 815, (1996).

[9] L.J. Rothberg, M.J. Yan, F. Papadimitrakopoulos, M.E. Galvin, E.W. Kwock, and T.M. Miller, Synth. Met. **80**, 41 (1996).

[10] T.W. Hagler, K. Pakbaz, K.F. Voss, and A.J. Heeger, Phys. Rev. B **44**, 8652 (1991).

[11] A.K. Sherdian, J.M. Lupton, I.D.W. Samuel, and D.D.C. Bradley, Chem. Phys. Lett. **322**, 51 (2000).

[12] See, for example, S. Adachi, *GaAs and Related Materials: Bulk Semiconducting and Superlattice Properties* (World Scientific, Singapore, 1994).

[13] Y.P. Varshni, Physica (Amsterdam) **34**, 149 (1967).

[14] L. Vina, S. Logothetidis, and M. Cardona, Phys. Rev. B **30**, 1979 (1984).

[15] P. Lautenschlager, M. Garriga, S. Logothetidis, and M. Cardona, Phys. Rev. B **35**, 9174 (1987).

[16] S. Guha, Q. Cai, M. Chandrasekhar, H.R. Chandrasekhar, H. Kim, A.D. Alvarenga, R. Vogelgesang, A.K. Ramdas, and M.R. Melloch, Phys. Rev. B **58**, 7222 (1998).

[17] P. Lautenschlager, P.B. Allen, and M. Cardona, Phys. Rev. B **31**, 2163 (1985).

[18] S. Tasch, A. Niko, G. Leising, and U. Scherf, Appl. Phys. Lett. **68**, 1090 (1996).

[19] S. Tasch, C. Brandstätter, F. Meghdadi, G. Leising, L. Athouel, and G. Froyer, Adv. Mater. **9**, 33 (1997).

[20] S. Setayesh, D. Marsitzky, and K. Müllen, Macromolecules **33**, 2016 (2000).

[21] K.N. Baker, A.V. Fratini, T. Resch, H.C. Knachel, W.W. Adams, E.P. Socci, and B.L. Farmer, Polymer **34**, 1571 (1993).

[22] S. Guha, W. Graupner, R. Resel, M. Chandrasekhar, H.R. Chandrasekhar, R. Glaser, and G. Leising, Phys. Rev. Lett. **82**, 3625 (1999).

[23] J. Grimme, M. Kreyenschmidt, F. Uckert, K. Müllen, and U. Scherf, Adv. Mater. **7**, 292 (1995).

[24] U. Scherf and E.J.W. List, Adv. Mater. **14**, 477 (2002).

[25] A.J. Cadby, P.A. Lane, H. Mellor, S.J. Martin, M. Grell, C. Giebeler, D.D.C. Bradley, M. Wohlgenannt, C. An, and Z.V. Vardeny, Phys. Rev. B **62**, 15 604 (2000).

[26] M. Grell, D.D.C. Bradley, X. Long, T. Chamberlain, M. Inbasekaran, E.P. Woo, and M. Soliman, Acta Polym. **49**, 439 (1998).

[27] G. Lieser, M. Oda, T. Miteva, A. Meisel, H.-G. Nothofer, U. Scherf, and D. Neher, Macromolecules **33**, 4490 (2000).

[28] E.J.W. List, C. Creely, G. Leising, N. Schulte, A.D. Schlüter, U. Scherf, K. Müllen, and W. Graupner, Chem. Phys. Lett. **325**, 132, (2000).

[29] E.J.W. List, R. Guentner, P.S. de Freitas, and U. Scherf, Adv. Mater. **14**, 374 (2002).

[30] T. Förster, Ann. Phys. (Leipzig) **2**, 55 (1948).

[31] A. Piaggi, G. Lanzani, G. Bongiovanni, A. Mura, W. Graupner, F. Meghdadi, G. Leising, and M. Nisoli, Phys. Rev. B **56**, 10 133 (1997).

[32] R. Kersting, B. Mollay, M. Rusch, J. Wenisch, G. Leising, and Kauffmann, J. Phys. C **106**, 2850 (1997).

[33] H. Bässler and B. Schweitzer, Acc. Chem. Res. **32**, 173 (1999).

[34] J. Brown, C. Elsass, C. Poblenz, P.M. Petroff, and I.S. Speck, Phys. Status Solidi B **228**, 199 (2001).

[35] C.F. Li, Y.S. Huang, L. Malikova, and F.H. Pollak, Phys. Rev. B **55**, 9251 (1997).